galaxies

MDPI

Article

Event Horizon and Environs (ETHER): A Curated Database for EHT and ngEHT Targets and Science

Venkatessh Ramakrishnan [1,2,*], Neil Nagar [2,*], Vicente Arratia [2], Joaquín Hernández-Yévenes [2], Dominic W. Pesce [3,4], Dhanya G. Nair [2], Bidisha Bandyopadhyay [2], Catalina Medina-Porcile [2], Thomas P. Krichbaum [5], Sheperd Doeleman [3,4], Angelo Ricarte [3,4], Vincent L. Fish [6], Lindy Blackburn [3], Heino Falcke [7], Geoffrey Bower [8] and Priyamvada Natarajan [3,4,9]

1 Finnish Centre for Astronomy with ESO, University of Turku, 20014 Turku, Finland
2 Astronomy Department, Universidad de Concepción, Barrio Universitario S/N, Concepción 4030000, Chile
3 Center for Astrophysics, Harvard & Smithsonian, 60 Garden Street, Cambridge, MA 02138, USA
4 Black Hole Initiative, Harvard University, 20 Garden Street, Cambridge, MA 02138, USA
5 Max Planck Institute for Radioastronomy, Auf dem Hugel 69, 53121 Bonn, Germany
6 Massachusetts Institute of Technology, Haystack Observatory, 99 Millstone Hill Road, Westford, MA 01886, USA
7 Department of Astronomy, Radboud Universiteit Nijmegen, 6525 AJ Nijmegen, The Netherlands
8 Academia Sinica Institute of Astronomy and Astrophysics, 645 N. A'ohoku Place, Hilo, HI 96720, USA
9 Department of Astronomy, Yale University, 52 Hillhouse Avenue, New Haven, CT 06511, USA
* Correspondence: venkatesshr@gmail.com (V.R.); nagar@astro-udec.cl (N.N.)

Abstract: The next generation Event Horizon Telescope (ngEHT) will observe multiple supermassive black hole (SMBH) candidates down to a few tens of mJy, and profoundly transform our understanding of the local SMBH population. Given the impossibility of large-area high-resolution millimeter surveys, multi-frequency spectral energy densities (SEDs), and models are required to both identify source samples tailored to specific science goals, and to predict the feasibility of detection of individual interesting sources. Here, we present the Event Horizon and Environs (ETHER) source and SED model database whose primary use is to enable the selection and optimization of targets for EHT and ngEHT science. The living ETHER database currently consolidates 1.6 million black hole mass estimates, ∼15,500 milliarcsec-scale radio fluxes, ∼14,000 hard X-ray fluxes (expected to grow by factor $\gtrsim$40 with the eROSITA data release) and SED information as obtained from catalogs and database queries, the literature, and our own new observations. Jet and accretion flow models are fit to individual SEDs in an automated way in order to predict the ngEHT observable fluxes from the jet base and accretion inflow. The database can be filtered by parameters or cross matched to a user source list, with the automated SED fitting models optionally fine tuned by the user. We have identified an initial ngEHT 'gold sample' for jet base studies and potentially black hole shadows; this sample will grow significantly in the coming years. While the ngEHT requires and will best exploit the ETHER database, six (eleven) ETHER sources have already been observed (scheduled) with the EHT in 2022 (2023), and the database has wide ranging applications in galaxy and black hole mass evolution studies.

Keywords: supermassive black holes; accretion inflows; jet launching; event horizon telescope; next-generation event horizon telescope; active galactic nuclei

Citation: Ramakrishnan, V.; Nagar, N.; Arratia, V.; Hernández-Yévenes, J.; Pesce, D.W.; Nair, D.G.; Bandyopadhyay, B.; Medina-Porcile, C.; Krichbaum, T.P.; Doeleman, S.; et al. Event Horizon and Environs (ETHER): A Curated Database for EHT and ngEHT Targets and Science. *Galaxies* **2023**, *11*, 15. https://doi.org/10.3390/galaxies11010015

Academic Editor: Bidzina Kapanadze

Received: 21 November 2022
Revised: 23 December 2022
Accepted: 26 December 2022
Published: 12 January 2023

1. Introduction

Supermassive black holes are believed to transition through 'hard' and 'soft' states [1]. Current theoretical models describe these states as arising from differences in the inner flow geometries. The latter are characterized by high accretion rates relative to Eddington, with emission in the inner 1000 gravitational radii; $R_g = GM/c^2$ where M is the BH mass dominated by UV to optical emission from an optically-thick geometrically-thin accretion

disk (10 s to 1000 s of gravitational radii) and X-rays from a 'corona' around the accretion disk. The 'hard' states reveal low Eddington accretion rates (low-luminosity active galactic nuclei or LLAGNs) and their radio to gamma-ray emission in the inner 1000 R_g comes primarily from a quasi-spherical accretion inflow in the innermost tens of R_g e.g., [2], and potentially from jets launched within 10 s of R_g. The innermost LLAGN accretion flows have been modelled with radiatively inefficient accretion flows (RIAFs), jets, or both e.g., [2–6]. The SMBH, when embedded in an accretion flow, or back-lit by a receding jet, produces a gravitationally-lensed bright ring with diameter 10.4 R_g [7], within which sits the shadow produced by its event horizon.

The next-generation event horizon telescope (ngEHT) will provide a spectacular increase in both sensitivity (detecting sources at $\sim$10 s of mJy), and native resolution (15 μarcsec) with super-resolution techniques potentially enabling resolutions of a few μarcsec. Additionally, the decreasing electron scattering with increasing frequencies and the often steeply increasing flux with frequency of the mm-wave emission from the inner accretion inflow, allows one to better resolve, or at least pinpoint accurately, the innermost region around the supermassive black hole as compared to cm-wave very long baseline interferometry (VLBI).

While the superlative sensitivity and resolution of the ngEHT will leverage wide ranging and transformational results in explicitly selected target samples, or in serendipitous sources of interest, it also creates a significant challenge. How do we identify and optimally select these few tens to thousands of ngEHT targets? Current predictions posit several to several thousand ngEHT detectable sources [8,9] with the range of predicted numbers depending on the still to be frozen technical specifications of the ngEHT. If we limit ourselves to SMBH with large black hole rings, e.g., within factor 5 of those in M87 and Sgr A*, we have only a few hundred potential targets, predominantly in the local universe. However, there are compelling reasons to include SMBHs with a large range of ring sizes. In terms of 'resolved' science, super-resolution techniques, future earth-space VLBI, and studies of jet launching at 10 s to 1000 s R_g, motivate the inclusion of SMBHs with ring sizes down to $\sim$1 μarcsec. Further, transformational science can be leveraged by using ngEHT-detected jets and accretion flows as 'signposts' independent of the linear resolution in scales of R_g, e.g., tracking orbits of binary SMBH. Direct selection of ngEHT targets is difficult for several reasons: (a) a sub-arcsec large-area survey at 230–345 GHz is curently impossible: for reference, a sub-arcsec ALMA 230 GHz survey of GOODS-S required $\sim$30 h to cover a 69 arcmin^2 area to a depth of 0.2 mJy/beam [10]. Observing the same area distributed over the sky is significantly more expensive due to calibration overheads; (b) all-sky mm-surveys have detection limits of a few hundred mJy, and resolutions of several arcminutes, e.g., Planck Collaboration et al. [11]; (c) multi-year large-area mm-surveys, e.g., SPT-3G [12] and JCMT-SCUBA2 [13], can only cover a few thousand of square degrees, at sensitivities of a few mJy to micro Jy, and resolutions of several tens of arcseconds to arcmin; and (d) dust is a strong contributor to 230–345 GHz emission, so that flux measurements at $\geq$ arcsec-scale are often dominated by galactic dust rather than the SMBH environment.

The few thousand ngEHT targets—which require to be bright ($\geq$few tens of mJy) and compact ($\lesssim$1000 R_g) at 230–345 GHz—are, thus, best pre-identified using SED fits on as large a sample of AGN and LLAGN possible. Posterior lower frequency VLBI and/or lower resolution 230 GHz imaging can then be used to confirm feasibility of ngEHT detection or imaging. For the first step, given the 'contamination' from host galaxy emission, one requires high resolution (ideally milliarcsec or mas scale, i.e., VLBI) flux measurements, and/or arcsec-scale fluxes at energies where the host galaxy is relatively faint, e.g., hard X-ray to γ-ray.

In this work, we present and describe the Event Horizon and Environment (ETHER) sample and database, which, independent of any specific science goal, aims to provide the definitive SMBH parent sample from which to select EHT and ngEHT targets in the

coming decades. Additionally, ETHER will offer an easy to use 'pipeline' to evaluate the observational feasibility of any given new source.

2. Materials and Methods

In this section, we describe the compilation of observational data which forms the basis of the ETHER database, the immediately derived quantities from these data, and the modelling procedure used to predict the ngEHT observing feasibility of any given source.

2.1. Catalogs and Data

Since the mass of a SMBH is one of its key physical and observable properties, ETHER compiles a mass estimate for every source in the database. This permits an estimate of the angular size of the black hole shadow and ring, constrains the scales (in terms of R_g) on which we can resolve the jet base, and is a necessary ingredient for the SED modelling. Only ∼230 galaxies have SMBH measurements, and we, thus, primarily depend on estimates. SMBH measurements, from stellar dynamics and ionized, molecular, and maser, gas kinematics, where available are taken from large compilations e.g., [14–16] individual publications, e.g., [17,18] and references therein, and online databases e.g., the Reverberation Mass (RM) database at http://www.astro.gsu.edu/AGNmass/ (accessed on 1 April 2020).

Our more reliable SMBH mass estimates come from the multiple black hole mass—host galaxy empirical scaling relationships, including that between SMBH mass and velocity dispersion (M-σ), or luminosity of the galaxy bulge (M-L_{bulge}), e.g., [15], 'single-epoch' reverberation mapping e.g., [19], and so-called 'fundamental planes' between SMBH mass and the pairs [effective radius of the bulge, central surface brightness]; e.g., Woo and Urry [20], [arcsec-scale radio and hard X-ray flux]; e.g., Gültekin et al. [21]. These scaling relationships are best calibrated at low redshifts and for SMBH masses $\gtrsim 10^7$ $M_\odot$ and we expect typical uncertainties of 0.3–0.6 dex in these. Here, velocity dispersions are from the HET massive galaxy survey [22], SDSS DR17 via astroqueries, and the Hyperleda database [23]. SMBH mass estimates from M-L_{bulge} are taken from Caramete and Biermann [24] and Mezcua et al. [25]. SMBH mass estimates from the following references—which use multiple methods—are also incorporated: Woo and Urry [20], Shaw et al. [26], Chen et al. [27].

If no black hole mass estimate is available from any of the above sources, we use WISE W1, W2, and W3 magnitudes from the AllWISE catalog [28] to derive a SMBH mass estimate (for details see Hernández-Yévenes, J., et al., in prep.). Briefly, the process is as follows: (a) WISE W1 and W2 band magnitudes are used to estimate the total stellar mass of the galaxy via Equation (2) of Cluver et al. [29]; (b) the WISE W2−W3 color is used to estimate the morphological type (T) of the galaxy. This color-morphological type relationship is trained on ∼25,000 galaxies with morphological classifications from the 2MRS catalog [30] and from NED[1] or SIMBAD; (c) the morphological type is used to estimate the bulge to total mass ratio following Figure 1 of Caramete and Biermann [24], and, thus, the bulge stellar mass, and (d) the SMBH mass estimate is derived using the $M_{BH} - M_{Bulge}$ relationship of Schutte et al. [31].

Two further corrections are applied to the WISE derived mass estimations. First, the WISE-derived mass shows small but systematic offsets to the values from the ∼230 ETHER galaxies with SMBH measurements and ∼400 ETHER galaxies with high-quality stellar velocity dispersion (thus high-quality SMBH estimation via the M-σ relationship). After empirically removing this offset the WISE-derived SMBH masses and the above mentioned ETHER SMBH masses (all in relatively nearby galaxies) agree within 0.6 dex. Second, powerful AGNs and ULIRGs are identified by their W2−W3 colors. In these, AGN emission could contaminate the W1 and W2 magnitudes, thus overestimating the SMBH mass. In these cases, we compare AGN bolometric luminosities with W3-derived total IR luminosities in order to flag those in which the AGN potentially contaminate the SMBH mass estimate from W1 and W2.

The details of the WISE based SMBH mass estimations will be presented in Hernández-Yévenes, J., et al., currently in preparation. While there are potentially large errors in individual values, statistically, these estimations are highly useful in the absence of any other. For example, this additional method provides us with SMBH mass estimates for a third of the VLBI-detected sources with no previous mass estimate, and 70% of the ∼520,000 ETHER galaxies at D $\leq$ 400 Mpc.

Redshifts and distances are incorporated from the original SMBH mass reference, or are taken, when necessary, from the Roma BZCAT 5th Ed. [32], the Veron-Cetty and Veron AGN catalog 13th Ed. [33], the Milliquas catalog [34], and via astroqueries to SIMBAD and NED. Luminosity and angular distances are derived from the EDD Database [35] for nearby ($\lesssim$50 Mpc) galaxies, or a standard flat cosmology with H_0 = 70 km/s, Omega$_m$ = 0.30, and Lambda$_0$ = 0.70.

High-resolution (mas-scale) radio fluxes come from the 2022b version of the RFC catalog[2], the VLBA calibrator list[3] , supplemented by 230 GHz EHT fluxes [5,6,36–38], 86 GHz GMVA fluxes [39,40], 43 GHz VLBA fluxes [41], 15 GHz VLBA fluxes [42], 5 GHz VLBA fluxes [43], NED and SIMBAD (via astroqueries), diverse literature results, and our ongoing VLBA and LBA programs (Ramakrishnan et al., in prep.). When mas-scale fluxes are not available, we use arcsec-scale fluxes from the 14 April 2022 version of the ALMA Calibrator catalog[4], from the literature for individual galaxies of interest, and from our own survey programs with ALMA (Nair et al., in prep.).

Hard X-ray fluxes are incorporated from NED photometry tables (via astroqueries) and the Chandra Source Catalogue (CSC) through the CSCview application [44]. Currently we have a total of 19,158 hard X-ray flux values, of which, 14,242 are high-resolution (∼1 arcsec) measurements.

Astroqueries to NED, SIMBAD, and SDSS are used to supplement information on position, redshift, SED fluxes, galaxy and AGN type, and galaxy size.

2.2. Models

The SED coverage, when considering only relatively high-resolution ($\lesssim$1 arcsec) measurements, is highly variable from source to source, is often sparse, and almost always non-simultaneous. We thus employ relatively simple analytical Advection Dominated Accretion Flow (ADAF) [8] and jet SED models [4,45] to predict fluxes at multiple frequencies (43, 86, 230, and 345 GHz) directly relevant to the EHT and ngEHT, or to our preliminary surveys aimed at selecting ngEHT targets. Details on these ADAF and/or jet model fits will be published in Arratia et al., in prep.

The analytic ADAF model is particularly useful for a large sample such as ETHER. While it internally uses many parameters, the total (synchrotron, bremsstrahlung, plus inverse Compton) ADAF SED is obtained by varying only the two most important variables—the SMBH mass and the Eddington ratio ($l_{\rm Edd}$; between 10^{-7} and $10^{-1.7}$). For the jet component, we currently use multiple (∼980) templates built from the models used in Bandyopadhyay et al. [4]. While this jet model has 15 free parameters, we only iterate over those that result in the most significant impact to the model SED, namely black hole mass, jet outflow rate, fraction of electrons accelerated in the shock, and the fraction of shock energy in these electrons. We are currently implementing a similar approach using the *BHJet* model [45], which has 26 free parameters, of which those that most effect the cm to hard X-ray SED include the black hole mass, viewing angle, injected power, and jet maximum extent.

To model the SED of an ETHER source (see, e.g., Figure 1), we require at least a distance or redshift, an SMBH mass estimate, and a hard X-ray flux. The Eddington rate is then varied until the the ADAF SED model fits the hard X-ray point. Errors in this estimate are based on errors of the black hole mass and hard X-ray flux.

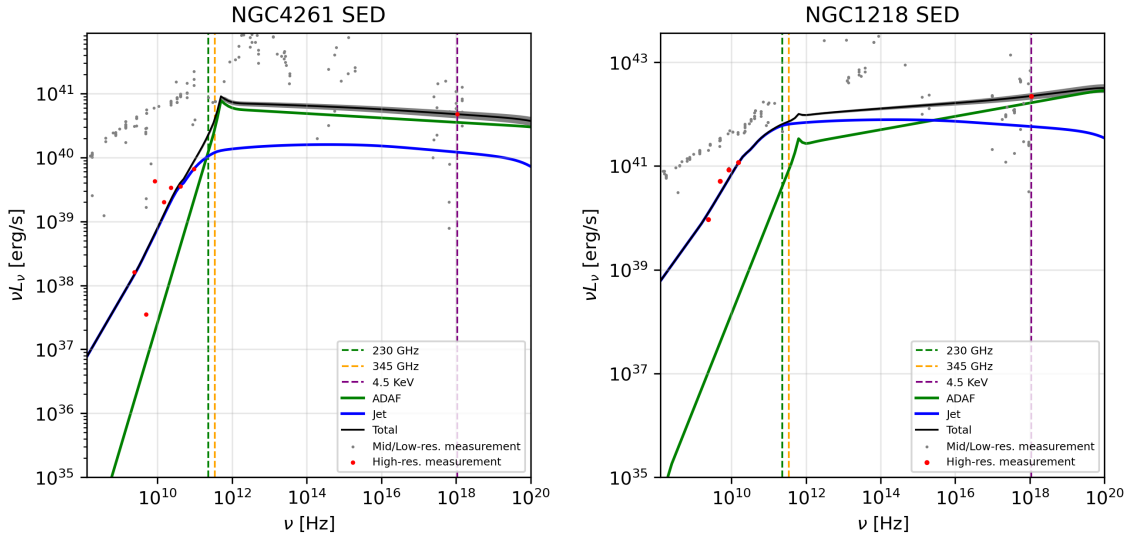

Figure 1. Spectral energy density plots contrasting two ETHER galaxies with known cm-wave nuclear jets: NGC 4261 (**left**) and NGC 1218 (3C 78; **right**). Red (grey) points indicate high (low) resolution flux measurements. For illustration, the cm-wave and hard X-ray data are fit with a scaled jet [4] and analytic ADAF model [8]. Vertical dotted lines indicate the current EHT observing frequency (230 GHz), and the hard X-ray band. For NGC 4261, the fitted jet component (blue) dominates at cm-waves while the ADAF component (green) is expected to dominate at 230 GHz. For NGC 1218, the jet is expected to dominate the 230 GHz EHT flux. We aim to systematically predict the EHT fluxes from the ADAF and jet base in ETHER galaxies using a SMBH mass estimate, hard X-ray flux (e.g., eROSITA), and, if a jet is present, high frequency VLBI observations. For SMBH with ring size ≥ 3 μarcsec, direct 230 GHz imaging with ALMA and SMA is also being pursued.

If one or more high resolution cm-wave fluxes are available, and these are, on average, above the ADAF-only model predictions, then a combined jet plus ADAF model is attempted. Here we attempt jet + ADAF fits with all of our current jet templates, and if multiple high resolution radio fluxes exist, we choose the fit with the lowest root-mean square (RMS) value between predicted and observed radio data. This combined jet plus ADAF fit to a given source thus primarily constrains the full range of expected fluxes from the jet and ADAF, rather than necessarily providing a single best-fit flux estimate plus its error.

Given the above caveats, and the fact that a hard X-ray flux is not currently available for many cm-wave VLBI sources in ETHER, Figures 2, 3 and 6 do not use fluxes derived from these model fits for VLBI-detected sources. Instead, for consistency and for illustration,the expected 230 GHz jet flux for the EHT is extrapolated from the the flux measured at the highest available VLBI frequency using the median spectral slope seen in our sample ($S_\nu \propto \nu^{-0.4}$), plus the median (from our sample) resolution factor which accounts for the smaller field of view as frequency increases.

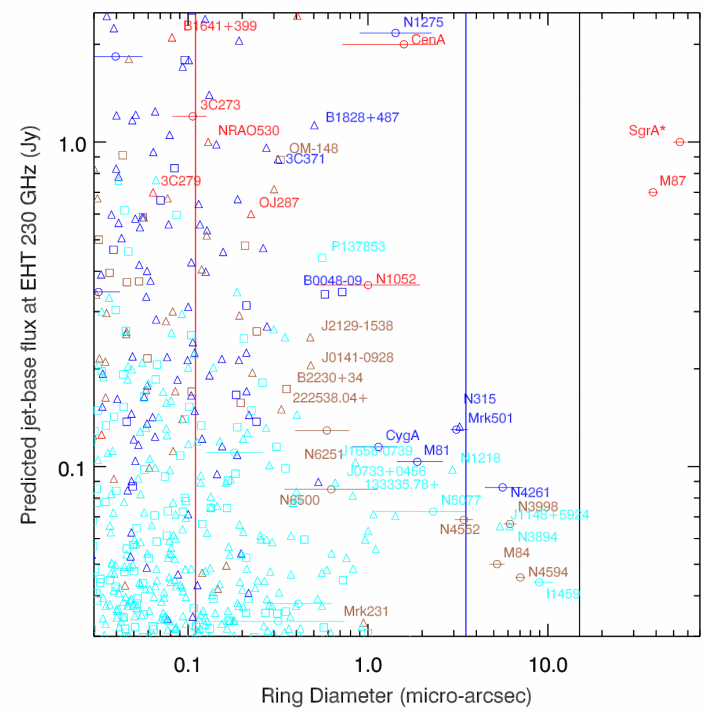

Figure 2. The estimated 0.1-mas-scale flux from the jet base when observed at 230 GHz with the EHT as a function of ring size (i.e., 10.4 R_g) for brighter VLBI-detected SMBH in ETHER. The intrinsic resolution of ground EHT, geostationary orbit to EHT, and L2 orbit to EHT will resolve the rings to the right of the black, blue, and red lines, respectively. Red, blue, and cyan symbols denote galaxies already observed with the EHT, with 43–86 GHz VLBI, and with <40 GHz VLBI, respectively. Circles (triangles) are used for SMBH mass measurements (estimations), and as a special case, our WISE-based SMBH mass estimations are shown with squares (see text).

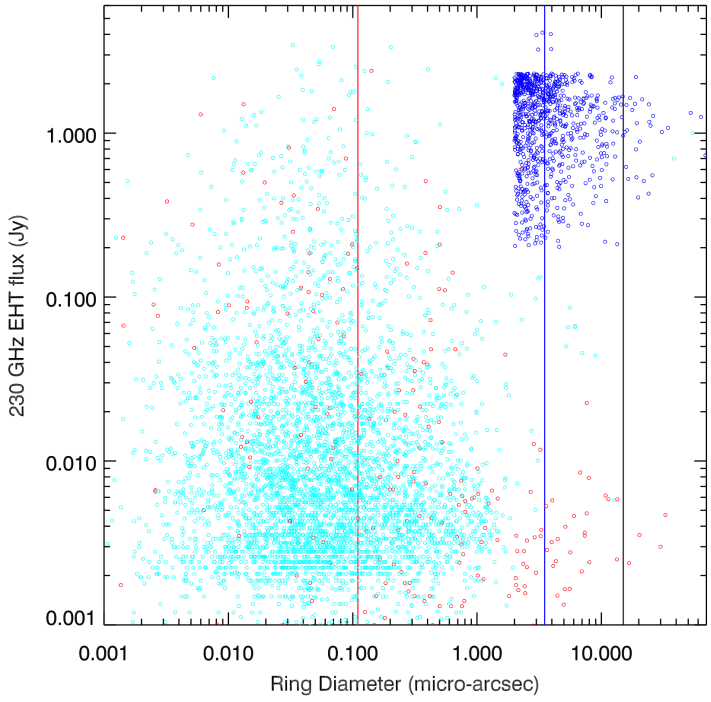

Figure 3. As in Figure 2 but this time with a larger axis range, and plotting additional SMBHs. The points of Figure 2 (VLBI-detected) are now all plotted as cyan circles: these represent the expected

flux from the jet base; the EHT flux will be higher if a significant ADAF component is present. For other SMBH, we plot the following fluxes, in order of availability: (a) SMBH with observed 230 GHz fluxes at arcsec-scales are plotted in red. No flux corrections for resolution are applied; (b) SMBH with observed-frame 230 GHz flux estimated from the ADAF-only models of Section 3.1.2 are plotted in green; (c) galaxies with an SMBH estimate, but none of the above, are plotted in blue *at an arbitrary y axis value*.

3. Results

3.1. ETHER: Overall Statistics

The ETHER sample (left panel of Figure 4) merges our collection of SMBH mass estimations, radio fluxes (VLBI, ALMA Calibrator database, literature, and our own work), of AGN and quasars identified in large catalogs (Section 2.1), and all ∼580 K galaxies in HyperLeda with Vrecc ≤ 25,000 km/s. Currently ETHER contains 1.9 million galaxies, of which 230 have a measured SMBH mass (from resolved stellar dynamics or gas kinematics), and ∼1.6 million have an indirectly derived estimate of the SMBH mass. The remaining galaxies are part of the sample due to being listed as an AGN or quasar in redshift catalogs, or for being a bright radio source, but are missing a redshift and/or a SMBH mass estimate. Of the 1.1 million SMBH estimations, 294 K are from M−σ, 290 K from WISE M-L_{bulge}, 5 K from other (non-WISE) M-L_{bulge}, and 500 K from single-epoch RM (primarily from [19]). Focusing on galaxies at D ≤ 300 Mpc, ETHER currently includes 77,000 galaxies with an SMBH estimate. The mass function of these, in shells of 20 Mpc width out to 290 Mpc is shown in the right panel of Figure 4. At D ≤ 100 Mpc our mass function is in agreement with the 'low' theoretical mass function adopted by Pesce et al. [8] except at the lowest masses. However, at larger distances we are increasingly incomplete at the low and higher mass ends. Ongoing SDSS-V (and future 4MOST) programs for spectroscopic observations of eROSITA sources, refinements of our WISE-derived SMBH mass estimates (Section 2.2) to lower signal to noise and/or W1-only detections, and the ingestion of further galaxy catalogs will help fill in this shortfall in the coming years.

Among the 15.4 K AGN detected with cm-wave VLBI, only 8.6 K have an SMBH mass measurement or estimate in ETHER. Of the remaining 6.8 K AGN, we do not currently have a redshift for 91%. Some fraction of these could be recovered with a more exhaustive ingestion of current literature and databases. Determining the missing redshifts and SMBH mass estimates, especially in the brighter VLBI sources, is a high priority in our future work.

Given an SMBH estimate, and a distance, we can estimate the diameter of the ring around the black hole: 10.4R_g [7].

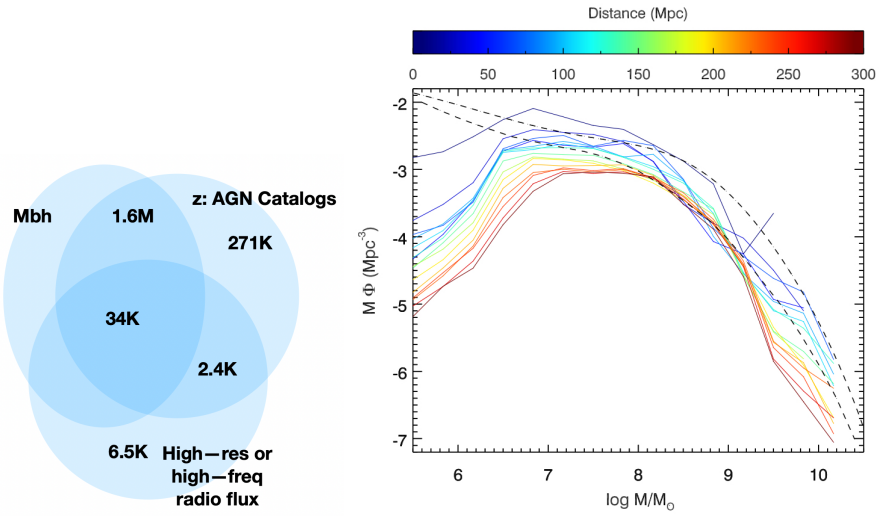

Figure 4. Left: summary statistics of the current ETHER sample. The number of SMBHs with black hole mass estimations, redshifts in AGN catalogs, and high (mas) resolution or high (≥230 GHz with

few to 20″ resolution) frequency radio fluxes are shown, together with their intersections. **Right**: the black hole mass function in ETHER for shells of width 20 Mpc at distances of 10 to 290 Mpc, following the color bar on top. For reference the z = 0 'low' and 'high' theoretical mass functions adopted by [8] are shown in dashed lines.

3.1.1. Jet Bases and Shadows

A major goal of the ngEHT is to study the physics of jet launching and collimation across the parameter space of, e.g., black hole mass, accretion rate, spin, and jet morphology at larger scales: here the ngEHT can uniquely constrain theoretical models in the innermost 10 s to 1000 s R_g e.g., [46]. For such goals, the optimal targets can be selected among the ∼15,400 AGN with already detected cm-wave VLBI cores. If an accretion inflow is present, or if the black hole is 'back-lit' by the receding jet base, then we can image, or constrain, the size of the black hole shadow and gravitationally lensed ring, in a subset of these jetted SMBH.

Figure 2 shows the expected EHT 230 GHz flux from the jet base (inner few 100 s of R_g) as a function of the linear resolution in R_g. Here, the expected EHT flux is illustrative. As we discuss in Section 2.2, we do model the combined jet and ADAF spectrum for AGN with cm-wave VLBI and hard X-ray fluxes. However, the bulk of the ETHER sample have one to few, non-simultaneous, VLBI flux measurements so that SED modelling is not an option for the overall sample. In Figure 2, for uniformity, we simplistically extrapolate the highest frequency VLBI flux to 230 GHz using the median (in our sample) spectral index of −0.4, plus a median (in our sample) flux dilution factor due to the increasing resolution with frequency (0.4–0.8 for 5–86 GHz)). Extrapolations from previous VLBI observations at ≥86 GHz (blue points in the figure) are thus more reliable than others (brown for 43 GHz measurements and cyan for lower frequencies—predominantly 8 GHz). Additionally, for illustration, in the case of Sgr A*—which currently has no detected jet emission—we use the flux of the accretion inflow.

Figure 2 clearly shows that Sgr A* and M87 are, unfortunately, relatively isolated in terms of large shadow size and bright EHT 230 GHz fluxes. While the blue and red lines in the figure delineate the limits for resolving the black hole ring for ngEHT to Geostationary orbit (ngEHT-Geo) satellite(s) and ngEHT to L2 orbit (ngEHT-L2) satellite(s), they also roughly represent the limits for resolving jet bases at 100 R_g and 1000 R_g, respectively, with a ground-based ngEHT. We, thus, already have ∼10 (few hundred) candidates in which the jet base can be resolved at better than 100 R_g (1000 R_g) with the ground-based EHT and ngEHT.

The 230 GHz EHT image of M87 Event Horizon Telescope Collaboration et al. [5] revealed that the flux in the innermost 100 s of R_g is dominated by the accretion inflow, rather than jet base (∼700 mJy in the bright ring produced by the gravitationally lensed accretion inflow, leaving only ∼300 mJy in the still-to-be-EHT-imaged jet base). This is also the scenario we expect from model fits to NGC 4261 (Figure 1); strong 230 GHz fringes detected on a ∼1000 km baseline in our March 2022 EHT observations of this source further supports this. Our current SED fits to other AGN to the right of the blue line in the figure favor the dominance of the accretion flow over the jet in most cases. Thus, as we pursue EHT imaging the the jet base in large ring, relatively low luminosity (as compared to Cen A, or even M87) jets, there is a large possibility that flux from the accretion inflow is detected in, and perhaps dominates, the EHT image in many cases. Super-resolution techniques could constrain black hole ring sizes in targets between the blue and black lines for a ground only ngEHT, and future ground to space VLBI can potentially resolve 10 s (100 s) of black hole rings if the accretion flow, or the receding jet-base, is bright enough.

Our current 'gold sample' of VLBI-detected jet bases includes 15 SMBHs (beyond Sgr A* and M87) with ring size ≥5 μarcsec, plus 39 SMBHs with ring size in the range 2–5 μarcsec. Based on current estimates and SED modelling, there is no reason to rule out

an ngEHT goal of constraining ∼5 to 10 black hole shadows, and imaging ∼10–20 jet bases at resolutions of a few tens of R_g.

While a true exploitation of this sample's potential requires the ngEHT, we have already commenced observations with the current EHT and GMVA+ALMA. All targets to the right of the blue line in Figure 2 were observed (imaging or fringe tests) in March 2022 with the EHT. All are scheduled be imaged with the GMVA+ALMA in March 2023, and an additional 11 SMBHs with ring diameter ≥1 μarcsec are scheduled for fringe-test observations (i.e., quick flux determinations) with the EHT in April 2023. Finally, since the March 2022 EHT observations of NGC 4261 showed strong fringes on a ∼1000 km baseline, a full track EHT observation of this is scheduled for April 2023.

It is relevant to mention the future growth of this jet-base sample. Currently, a third of cm-wave VLBI detected sources in ETHER lack redshifts. An additional 20% lack a SMBH mass estimate: assuming a M87-like SMBH for these latter yield shadow sizes primarily in the range ∼0.1–3 μarcsec. Finally, several VLBI compilations in the literature remain to be ingested into ETHER. The number of potential jet base targets appearing in this figure is thus expected to increase by factor up to two in the coming years, through black hole mass estimates from large surveys, e.g., SDSS-V and 4MOST, and with our own programs. Our programs to obtain higher frequency VLBI (including EHT) observations of the best targets here will allow improvements in our SED model procedure and, thus, 230 GHz flux estimations, and lead to a larger and more reliably identified 'gold' sample for the ngEHT.

As our parent sample increases, we require more efficient pathways to confirm model-selected ngEHT targets. Sources with large ring size and promising jet + ADAF fits to observed fluxes at $\nu < 43$ GHz, are currently being followed up with 43 GHz VLBA snapshot imaging. The combination of 43 GHz VLA and 230 GHz ALMA (or ALMA-ACA) can efficiently survey several hundreds of sources and identify those with 'sub-mm' bumps from the ADAF. Snapshot imaging with the (phased-reference) VLBA at 43 GHz or with GMVA+ALMA can then further filter this sample before ngEHT fringe tests are attempted.

3.1.2. ETHER: Accretion Flows

The absence of a bright radio jet does not necessarily imply the absence of a EHT-detectable accretion inflow (Section 1). Pesce et al. [8] posit that massive ($\geq 10^{9.5}$ $M_\odot$), high accretion rate ($\log l_{\rm Edd} \sim -1.7$ to -3) SMBHs have the most luminous accretion inflows at 230 GHz. These extreme objects are not in the 'low-hard' state, and may not launch powerful jets (Section 1). We thus require to identify 230 GHz bright accretion flow sources independent of the presence of a radio jet or a previous cm-wave VLBI detection of this. It would not be at all surprising if such accretion-inflow-only ngEHT targets eventually outnumber ngEHT targets selected via the presence of VLBI jets (Section 3.1.1). Resolving accretion inflows allow us to access resolved shadows and rings, to obtain constraints on competing accretion models (e.g., MAD or SANE), and detect orbiting hotspots. Detected unresolved accretion inflows are highly useful signposts for other science cases (Section 3.1.3).

We are following two pathways towards identifying accretion-inflow-only ngEHT targets. First, the largest known black hole rings. ETHER currently includes 623 (85) SMBHs with estimated ring diameters ≥3 μarcsec (≥10 μarcsec), independent of the presence of a VLBI-detected jet. These 623 SMBHs are either in relatively nearby (D ≤ 100 Mpc) galaxies, in central galaxies of galaxy clusters at $z \lesssim 0.3$, or massive broad-line SMBHs at higher redshifts from Rakshit et al. [19]. We are in the process of directly measuring the arcsec-scale 230 GHz flux in all of these. Between the literature and calibrator databases (∼30 SMBHs), our ALMA-ACA programs in the last two years (∼130 SMBHs), and programs proposed to the SMA (currently ∼100 SMBHs), we are less than half-way through this process, though new candidates are added as ETHER grows. Leaving aside VLBI detected galaxies (addressed in Section 3.1.1), we have thus far detected 35 targets with 230 GHz fluxes between ∼1 and 22 mJy at resolutions of 1″ to 5″. The remaining are not detected at 3σ upper limits of ∼1–2 mJy. The detected sources require to be observed at higher resolution

(e.g., ∼50 mas with the ALMA 12 m array), before clearer statistics, and a 'gold sample' emerge. Further, we are still highly incomplete in large diameter rings (Figure 4) even in the local universe, so this sample of large rings without jets is expected to grow significantly in the coming years (see below).

Second, for future larger samples of large ring SMBHs, and ngEHT-bright accretion flow SMBHs across all ring diameters, direct arcsec-resolution all-sky mm surveys to identify the few hundreds of EHT science targets are impossible (Section 1). While detailed 1-D models, e.g., [4] and full GRMHD models, e.g., [47] of the accretion inflow exist, applying these to millions of SMBH with sparse data is currently not feasible. We, thus, commence with the relatively simple analytical model of Pesce et al. [8] which requires only two user parameters—SMBH mass and accretion rate—to predict the combined synchrotron, inverse Compton, and thermal emission from the accretion inflow (see Section 2). High-resolution data points at frequencies higher than mm-wave are best used to constrain the ADAF SED, since cm-wave fluxes are dominantly from the jet and other galaxy components. Hard X-ray fluxes are an ideal solution since even at resolutions of 1–10″ the bulk of the emission is expected to come from the SMBH environs, and for $\log l_{\rm Edd} \lesssim -2$ it is likely that a significant fraction of this originates in the accretion inflow rather than a corona.

Currently, we have hard X-ray fluxes and SMBH mass estimates for ∼16,800 ETHER galaxies. We fit analytical ADAF models to all of these in order to predict the 43 to 345 GHz fluxes from the ADAF. Figure 5 shows preliminary results of our observed 230 GHz fluxes (red and blue points) and predicted 230 GHz fluxes from the ADAF fits (green points) and compare them with the ADAF fluxes predicted from the analytic models for three specific (and one illustrative) SMBHs over a range of redshifts. We should immediately note that most high redshift 230 GHz fluxes are ALMA Calibrator Database flux measurements of known cm-wave VLBI sources (blue points in the figure). In most of these we expect that the jet, rather than accretion inflow, dominates the 230 GHz flux, and this is borne out by our SED model fits. Even when we assume that all the hard X-ray flux originates in the ADAF the predicted 230 GHz ADAF fluxes are significantly lower than the measured arcsec-scale fluxes. These bright jet sources are thus best modelled with a combined jet plus ADAF model, though an additional complication is contamination from dust emission in the 1 to 5″ beam of the 230 GHz flux measurements.

At $D \leq 400$ Mpc, we see a larger overlap between arcsec-scale measured and mas-scale ADAF-predicted 230 GHz fluxes. In the few test cases where the mm-wave flux is measured at sub-arcsec resolution, and there is no indication of a cm-wave jet, we obtain a factor ∼5 agreement. We clearly require a larger sample of jet-free, or weak-jet, cases to best determine the precision of our ADAF-only estimates. Our ongoing ALMA (and proposed SMA) programs to observe large-ring galaxies without evidence for cm-wave jets (see above), together with hard X-ray fluxes from eROSITA will increase our test sample size by factor $\gtrsim$10–100 and allow refinements and consistency tests in these model predictions. Future improvements also include the use of SEDs from full (scaled) GRMHD modelling of accretion inflows, and/or fine tuning of the Pesce et al. [8] models.

Our identification of accretion-inflow-only bright targets for the ngEHT is very much at an initial stage. Current results favor the requirement of a ngEHT detection threshold of a few mJy, even for studies of unresolved accretion inflows. However, there are several reasons we expect the sample to expand by factor ∼10 to 50. First, eROSITA expects to detect ∼1 million hard X-ray sources in their all sky survey (first data release scheduled for March 2023), with ongoing SDSS-V and future 4MOST spectroscopic follow-ups to determine black hole masses of eROSITA detections. Massive SMBHs with relatively high accretion rates are expected to have ADAFs bright in both the hard X-ray and at 230 GHz (see above and [8]), so that the eROSITA selection, and posterior SED modelling with ADAFs, is an especially promising pathway to select ngEHT targets in the coming years. Further, our current ETHER SMBH mass function (Figure 4) remains incomplete at the high mass end, even in the local universe. Filling in this deficit, via additional WISE- and

2MASS-derived SMBH estimates, plus other (and ours) spectroscopic and photometric programs, will allow an increase in our target samples.

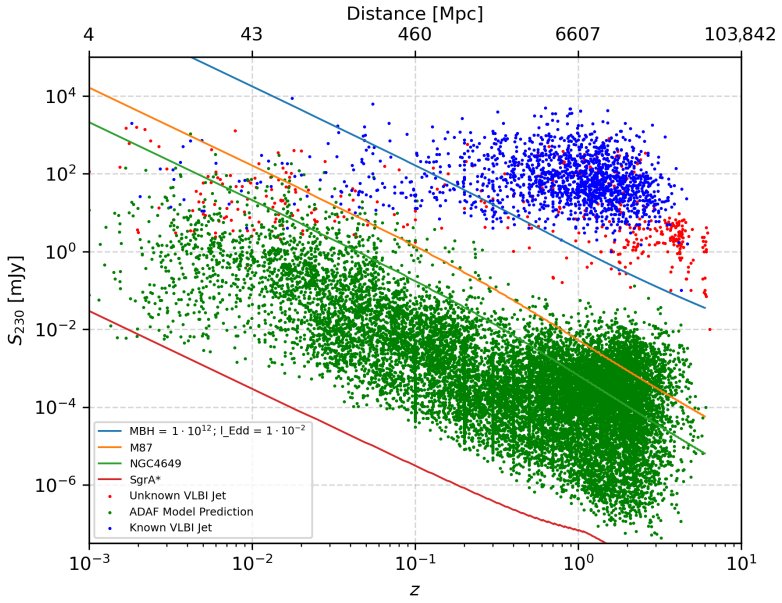

Figure 5. Measured (red and blue points) and model-predicted (green points) 230 GHz fluxes as a function of redshift (lower axis) and distance (upper axis). Blue points are used for SMBH with known cm-wave VLBI detections, i.e., AGN with compact jets. Green points show the expected flux from the analytic model of Pesce et al. [8] given our SMBH mass estimate and a measured hard X-ray flux (presumed to come only from the ADAF). The evolution of the ADAF flux with redshift—using the Pesce et al. [8] models—for SgrA*, M87, and NGC4649, and an illustrative extreme high-mass high-accretion-rate SMBH—are shown in colored lines following the legend on the panel. Details can be found in Arratia et al., in prep.

3.1.3. ETHER: Other Science Cases

The ngEHT will pursue several science cases in varied targets independent of their linear resolution in R_g scales, e.g., using the emission from the jet base and/or accretion inflow as signposts (e.g., the search for resolved binary supermassive black holes in their gravitational emitting phase) or to better constrain multi-wavelength and multi-messenger phenomena.

Figure 6 shows the predicted 230 GHz EHT flux (the same extrapolation used in Figure 2) but this time as a function of linear resolution at the redshift of the SMBH. The EHT has a sub-0.2 pc resolution across the universe, and can uniquely resolve binary SMBHs during their gravitation wave emitting inspiral. Here we once more only plot VLBI-detected SMBHs and use an estimated flux of the jet base. The future addition of additional VLBI-detected SMBHs and also bright ADAF-only sources will significantly increase the number of SMBHs in this figure.

There are currently ∼160 binary SMBH candidates in ETHER, as identified by diverse methods for a review, see [48]. Only about 10, e.g., [49–51] come from direct VLBI imaging of multiple potential SMBHs. The majority of posited binary SMBHs come from the interpretation of periodic flux variability, e.g., [52,53], double velocity components in the Narrow, e.g., [54] or Broad, e.g., [55] line region. X-shaped radio sources are also candidates [56]: while the X-shape can be explained by the characteristics of the spin axis of a single SMBH, they could also potentially be produced by binary SMBH. Additionally, Ref. [57] have identified the nearby galaxies most likely to host binary SMBHs based on simulating their merger history.

An analysis similar to that of single SMBHs in ETHER, but including a statistical treatment of the SMBH mass ratio, is being used to select the best candidates for ngEHT

monitoring surveys. The Vera C. Rubin Observatory will enable extensive studies of periodic flux variability, and is thus expected to significantly enlarge the sample of binary black hole candidates. The ETHER database will provide a pathway towards identifying the subset of these which are best observable with the ngEHT.

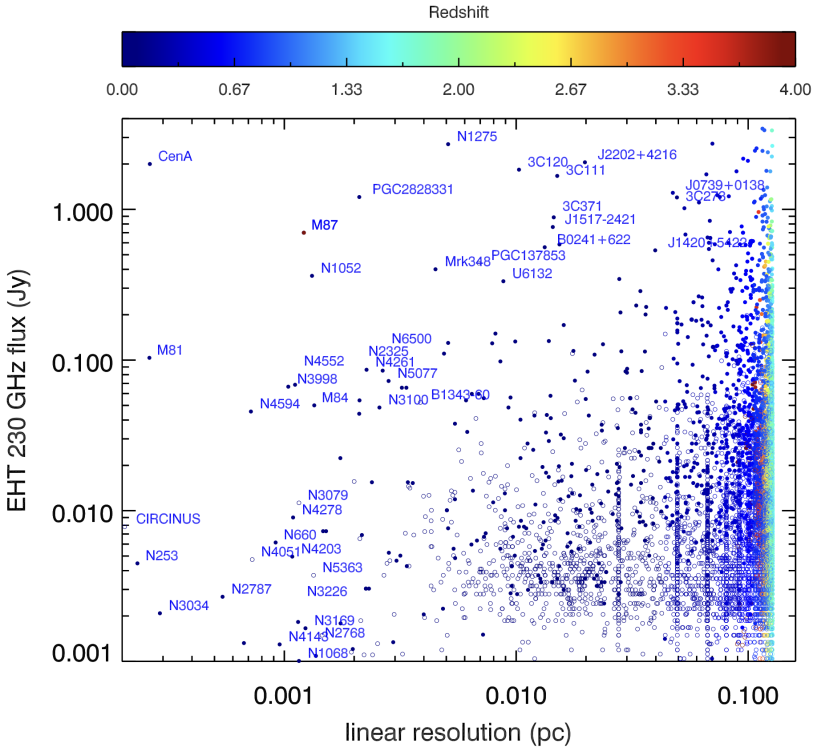

Figure 6. The estimated 230 GHz flux from the jet base—for VLBI detected sources only—as a function of linear resolution of the EHT assuming a 15 μarcsec angular resolution: the EHT has a sub 0.2 pc resolution across the universe. EHT-Geo and EHT-L2 baselines would increase this by factor $\sim$4 and $\sim$130, respectively. Symbols are colored by redshift following the color bar, and some individual galaxies are named in uncrowded regions of the plot. Vertical striations are primarily due to redshifts with few significant digits in Véron-Cetty and Véron [33]. We expect to add a significant number of additional sources on this plot, both from new cm-VLBI detections, and for AGN with a bright accretion inflow.

3.2. ETHER: Querying and Usage

The ETHER database and server is currently being prepared for release on a dedicated server via a *Python* interface. The tabulated searchable data will include: (a) basic source data including position, distance, redshift, AGN type, galaxy morphological type; (b) the best available (and the WISE-based) black hole mass estimate, plus errors and quality flags, the estimated shadow size and linear resolution at the SMBH angular distance, the estimated stellar mass and star formation rate, and the AGN bolometric luminosity; (c) fluxes at all typical VLBI frequencies, and at hard X-ray and γ-ray; and (d) model predicted ADAF-only and jet and ADAF fluxes at ngEHT frequencies. For proper attribution of credit, all user outputs will contain easy-to-use references (in 'bibtex' and equivalent formats) for data ingested from the literature or other databases. Each source will additionally link to files containing its full SED data, and the model parameters and SEDs of the best-fit ADAF and jet+ADAF models.

The database interface will support two types of usage: (a) cross-matching to a list of names or positions. This interface will match targets to the existing database and return tabulated data, model results, and figures. In case input positions are not matched to the database, the server will generate *Python*-based 'astro-queries' to relevant databases and

virtual observatories, run relevant models, and incorporate the new data into the database and the returned results; and (b) exploration of the current database, using a GUI with multi-parameter filters in order to obtain specific sub-samples of science targets.

In the future, the database will be interfaced to other ngEHT simulation tools currently in development, so that observing constraints and optimizations can be taken into account when choosing a final sample.

4. Discussion

Figure 3 combines the results of our previous sections to show a more comprehensive view of (the current status of) the ngEHT target pool. We emphasize that this figure is illustrative and preliminary: many data-points in the figure come from low-resolution fluxes, model predictions, and extrapolations still undergoing refinement. On the positive side, our parent sample will grow significantly in the coming years (we expect a factor at least two for jet sources and factor ∼10–50 for accretion-only inflow sources, see Sections 3.1.1 and 3.1.2).

Jet-base targets for the EHT (cyan circles)—whose brighter subset are seen in more detail in Figure 2—primarily cluster at expected EHT 230 GHz fluxes of 2 to 30 mJy, and expected ring diameters of 0.005 to 0.5 μarcsec. While these are identified via their cm-wave VLBI jet emission, note that in M87 the EHT showed that the 230 GHz nuclear emission is dominated by accretion inflow rather than jet base [5]. Remaining SMBHs with observed arcsec-scale resolution 230 GHz fluxes are shown in red. Here, those at smaller ring sizes are primarily bright sources from the ALMA Calibrator database (and likely dominated by jet emission at 230 GHz) but also include weaker sources: those at the largest ring sizes come primarily from our ongoing ALMA-ACA programs to directly measure 230 GHz fluxes. In the latter, the ∼5 arcsec resolution of ALMA-ACA means that the fluxes are potentially contaminated by dust from the host galaxy, so future ∼50 mas resolution ALMA observations of the brighter detections will be required to confirm their ADAF origin. For several hundred SMBH with large ring sizes, we currently do not have an accurate path towards estimating 230 GHz fluxes. Those at estimated ring sizes ≥ 2 μarcsec are shown as blue circles (with an arbitrary flux value in the y axis in Figure 2): the number of these SMBH increases rapidly below this ring size but we do not show them to avoid crowding on the plot. These SMBH—divided roughly equally between nearby galaxies and high-z galaxies with large SMBH mass estimates from Rakshit et al. [19]—are the targets of our ongoing ALMA/ACA and SMA (proposed) programs. Finally, SMBH with 230 GHz fluxes predicted from our ADAF-only models are shown with green. Currently, these cluster at predicted fluxes of $\lesssim$10 mJy.

The cumulative histograms of ring sizes in the current ETHER sample are shown in the right panel of Figure 7. While the cumulative distribution (red) shows >10 rings already resolvable, in principle, by the EHT, and rises quickly to smaller shadows, the subset previously detected at mas-scales at $\nu > 40$ GHz (primarily jet-base candidates) significantly lags behind. Two factors contribute to this effect: (a) intrinsically weak radio emission at all frequencies from the innermost SMBH environs—as evidenced by across the board low fluxes at lower spatial resolutions, and (b) the lack of high resolution—and in many cases any resolution—mm-wave observations of many sources. In these sources, weak cm-wave fluxes (from a jet base) does not necessarily imply weak mm-wave fluxes (from the accretion inflow). As described in the previous sections, we are actively attempting to mitigate the second factor. Further, flux monitoring of SMBH in the former sub-class may reveal new targets due to variability, which is not uncommon in the mm [58].

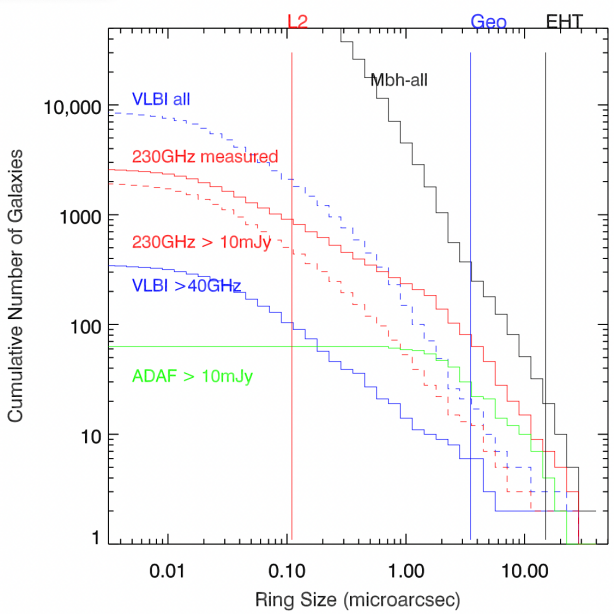

Figure 7. Cumulative histograms of 'ring' sizes in the ETHER sample. The intrinsic 15 μarcsec resolution of ground EHT, geostationary orbit to EHT, and L2 orbit to EHT at 345 GHz will resolve the rings to the right of the black, blue, and red lines, respectively. The cumulative histogram of all 230 GHz flux measurements, and all 230 GHz flux measurements greater than 10 mJy, are shown with the red solid and dashed lines, respectively.

The cumulative distribution of detectable accretion inflows (ADAFs) remains to be determined, as we are in the initial phase of this pathway (see above, and Section 3.1.2). The cumulative distribution of sources with measured or expected flux $\geq$ 10 mJy are shown in red. These should be treated with caution: the number of AGN with 230 GHz fluxes predicted from hard X-ray fluxes and ADAF models will increase by factor $\sim$100 with eROSITA and SDSS-V, while the current measured 230 GHz fluxes will likely decrease as higher resolution observations are obtained. The cumulative histogram of sources with measured 230 GHz flux smaller than 10 mJy is shown in green. Clearly, even at large black hole ring sizes, the many targets lack a 230 GHz measured flux, at any resolution, or a flux prediction via ADAF models. Our ongoing ALMA, and proposed SMA, programs aim to obtain fluxes for all with estimated ring size $\geq$ 2 μarcsec.

The millions of black hole mass estimates used in ETHER come from diverse methods, including our automated WISE-based estimations, with varying random and systematic errors. Detailed manual analysis of existing data, and new data, will be (and is being) used to refine these black hole mass estimates for specific targets which enter our ngEHT 'Gold Samples'.

In conclusion, the ETHER sample and database consolidates data and model predictions of all potential ngEHT candidates independent of science case. It also provides pathways towards determining the factability of ngEHT observations of any given new source. While we expect the sample to expand significantly (factor $\sim$10–50 for accretion-inflow-only targets, and $\sim$2 for known cm-wave VLBI jets) we have already identified a 'gold sample' for ngEHT jet base and potentially black hole shadow studies, and have commenced to observe these with the existing EHT.

Author Contributions: Conceptualization, V.R., N.N., D.W.P., T.P.K., S.D., H.F., G.B. and P.N.; Data curation, V.R., N.N., V.A., J.H.-Y., D.G.N., V.L.F., L.B. and G.B.; Funding acquisition, N.N., S.D. and H.F.; Investigation, V.R., N.N., V.A., J.H.-Y., D.G.N., B.B., C.M.-P., V.L.F. and P.N.; Methodology, V.R., N.N., D.W.P., B.B., T.P.K., S.D., A.R., V.L.F., L.B., H.F., G.B. and P.N.; Project administration, V.R. and N.N.; Resources, V.R., S.D., V.L.F., L.B. and H.F.; Software, N.N., V.A., J.H.-Y., D.W.P., B.B. and L.B.; Supervision, N.N.; Validation, N.N., V.A. and C.M.-P.; Writing—original draft, V.R. and N.N.; Writing—review & editing, V.A., J.H.-Y., D.W.P., T.P.K., A.R. and P.N. All authors have read and agreed to the published version of the manuscript.

Funding: We acknowledge funding from ANID Chile via Nucleo Milenio TITANs (Project NCN19-058), Fondecyt Regular (Project 1221421), Fondecyt Postdoctorado (Project 3220195) and BASAL (Projects AFB-170002 and FB210003).

Data Availability Statement: The ETHER database will be available at www.titans.cl/ether (accessed on 8 March 2020).

Acknowledgments: This paper makes use of ALMA data. ALMA is a partnership of ESO (representing its member states), NSF (USA) and NINS (Japan), together with NRC (Canada), MOST and ASIAA (Taiwan), and KASI (Republic of Korea), in cooperation with the Republic of Chile. The Joint ALMA Observatory is operated by ESO, AUI/NRAO and NAOJ. We acknowledge the usage of the HyperLeda database (http://leda.univ-lyon1.fr; accessed on 8 March 2020 for all galaxy velocity dispersions, and on 29 November 2022 for the list of all D $\leq$ 350 Mpc galaxies), and congratulate its managers for the easy to use interface provided. This research has made use of the NASA/IPAC Extragalactic Database (NED), which is funded by the National Aeronautics and Space Administration and operated by the California Institute of Technology. This research has made use of the SIMBAD database, operated at CDS, Strasbourg, France. This research has made use of the VizieR catalogue access tool, CDS, Strasbourg, France. This research was supported in part by the Black Hole Initiative, which is supported by grants by the Gordon and Betty Moore Foundation and John Templeton Foundation. The opinions expressed in this publication are those of the author(s) and do not necessarily reflect the views of the Moore or Templeton Foundations.

Conflicts of Interest: The authors declare no conflict of interest.

Abbreviations

The following abbreviations are used in this manuscript:

ADAF	Advection Dominated Accretion Flow
EHT	Event Horizon Telescope
ETHER	Event Horizon and Environs Sample
ngEHT	next-generation Event Horizon Telescope
SMBH	supermassive black hole(s)

Notes

1 The NASA/IPAC Extragalactic Database (NED) is funded by the National Aeronautics and Space Administration and operated by the California Institute of Technology.

2 http://astrogeo.org/rfc/ (accessed on 5 February 2021).

3 http://www.vlba.nrao.edu/astro/calib/ (accessed on 5 February 2021).

4 https://almascience.eso.org/alma-data/calibrator-catalogue (accessed on 5 February 2021).

References

1. Yuan, F.; Narayan, R. Hot Accretion Flows around Black Holes. *Annu. Rev. Astron. Astrophys.* **2014**, *52*, 529–588.
2. Narayan, R.; Yi, I.; Mahadevan, R. Advection-Dominated Accretion Model of Sagittarius A* and Other Accreting Black Holes. *Astron. Astrophys. Suppl.* **1996**, *120*, 287–290.
3. Markoff, S.; Bower, G.C.; Falcke, H. How to hide Large-Scale Outflows: Size Constraints on the Jets of Sgr A*. *Mon. Not. R. Astron. Soc. Lett.* **2007**, *379*, 1519–1532.
4. Bandyopadhyay, B.; Xie, F.G.; Nagar, N.M.; Schleicher, D.R.G.; Ramakrishnan, V.; Arévalo, P.; López, E.; Diaz, Y. Resolving Accretion Flows in Nearby Active Galactic Nuclei with the Event Horizon Telescope. *Mon. Not. R. Astron. Soc. Lett.* **2019**, *490*, 4606–4621.

5. Event Horizon Telescope Collaboration; Akiyama, K.; Alberdi, A.; Alef, W.; Asada, K.; Azulay, R.; Baczko, A.K.; Ball, D.; Baloković, M.; Barrett, J.; et al. First M87 Event Horizon Telescope Results. I. The Shadow of the Supermassive Black Hole. *Astrophys. J. Lett.* **2019**, *875*, L1.
6. Event Horizon Telescope Collaboration; Akiyama, K.; Alberdi, A.; Alef, W.; Algaba, J.C.; Anantua, R.; Asada, K.; Azulay, R.; Bach, U.; Baczko, A.K.; et al. First Sagittarius A* Event Horizon Telescope Results. I. The Shadow of the Supermassive Black Hole in the Center of the Milky Way. *Astrophys. J. Lett.* **2022**, *930*, L12. [CrossRef]
7. Johannsen, T.; Psaltis, D. Testing the No-hair Theorem with Observations in the Electromagnetic Spectrum. II. Black Hole Images. *Astrophys. J.* **2010**, *718*, 446–454.
8. Pesce, D.W.; Palumbo, D.C.M.; Narayan, R.; Blackburn, L.; Doeleman, S.S.; Johnson, M.D.; Ma, C.P.; Nagar, N.M.; Natarajan, P.; Ricarte, A. Toward Determining the Number of Observable Supermassive Black Hole Shadows. *Astrophys. J.* **2021**, *923*, 260.
9. Pesce, D.W.; Palumbo, D.C.M.; Ricarte, A.; Broderick, A.E.; Johnson, M.D.; Nagar, N.M.; Natarajan, P.; Gómez, J.L. Expectations for Horizon-Scale Supermassive Black Hole Population Studies with the ngEHT. *Galaxies* **2022**, *10*, 109. [CrossRef]
10. Franco, M.; Elbaz, D.; Béthermin, M.; Magnelli, B.; Schreiber, C.; Ciesla, L.; Dickinson, M.; Nagar, N.; Silverman, J.; Daddi, E.; et al. GOODS-ALMA: 1.1 mm Galaxy Survey. I. Source Catalog and Optically Dark Galaxies. *Astron. Astrophys.* **2018**, *620*, A152.
11. Planck Collaboration; Ade, P.A.R.; Aghanim, N.; Argüeso, F.; Arnaud, M.; Ashdown, M.; Aumont, J.; Baccigalupi, C.; Banday, A.J.; Barreiro, R.B.; et al. Planck 2015 results. XXVI. The Second Planck Catalogue of Compact Sources. *Astron. Astrophys.* **2016**, *594*, A26.
12. Sobrin, J.A.; Anderson, A.J.; Bender, A.N.; Benson, B.A.; Dutcher, D.; Foster, A.; Goeckner-Wald, N.; Montgomery, J.; Nadolski, A.; Rahlin, A.; et al. The Design and Integrated Performance of SPT-3G. *Astrophys. J. Suppl. Ser.* **2022**, *258*, 42.
13. Simpson, J.M.; Smail, I.; Swinbank, A.M.; Chapman, S.C.; Chen, C.C.; Geach, J.E.; Matsuda, Y.; Wang, R.; Wang, W.H.; Yang, Y.; et al. The East Asian Observatory SCUBA-2 Survey of the COSMOS Field: Unveiling 1147 Bright Sub-Millimeter Sources across 2.6 Square Degrees. *Astrophys. J.* **2019**, *880*, 43.
14. van den Bosch, R.C.E. Unification of the Fundamental Plane and Super Massive Black Hole Masses. *Astrophys. J.* **2016**, *831*, 134.
15. Saglia, R.P.; Opitsch, M.; Erwin, P.; Thomas, J.; Beifiori, A.; Fabricius, M.; Mazzalay, X.; Nowak, N.; Rusli, S.P.; Bender, R. The SINFONI Black Hole Survey: The Black Hole Fundamental Plane Revisited and the Paths of (Co)evolution of Supermassive Black Holes and Bulges. *Astrophys. J.* **2016**, *818*, 47.
16. Thater, S.; Krajnović, D.; Cappellari, M.; Davis, T.A.; de Zeeuw, P.T.; McDermid, R.M.; Sarzi, M. Six New Supermassive Black Hole Mass Determinations from Adaptive-Optics Assisted SINFONI Observations. *Astron. Astrophys.* **2019**, *625*, A62.
17. Boizelle, B.D.; Walsh, J.L.; Barth, A.J.; Buote, D.A.; Baker, A.J.; Darling, J.; Ho, L.C.; Cohn, J.; Kabasares, K.M. Black Hole Mass Measurements of Radio Galaxies NGC 315 and NGC 4261 Using ALMA CO Observations. *Astrophys. J.* **2021**, *908*, 19.
18. North, E.V.; Davis, T.A.; Bureau, M.; Cappellari, M.; Iguchi, S.; Liu, L.; Onishi, K.; Sarzi, M.; Smith, M.D.; Williams, T.G. WISDOM project—V. Resolving Molecular Gas in Keplerian Rotation around the Supermassive Black Hole in NGC 0383. *Mon. Not. R. Astron. Soc. Lett.* **2019**, *490*, 319–330.
19. Rakshit, S.; Stalin, C.S.; Kotilainen, J.; Shin, J. High-Redshift Narrow-Line Seyfert 1 Galaxies: A Candidate Sample. *Astrophys. J. Suppl. Ser.* **2021**, *253*, 28.
20. Woo, J.H.; Urry, C.M. Active Galactic Nucleus Black Hole Masses and Bolometric Luminosities. *Astrophys. J.* **2002**, *579*, 530–544.
21. Gültekin, K.; King, A.L.; Cackett, E.M.; Nyland, K.; Miller, J.M.; Di Matteo, T.; Markoff, S.; Rupen, M.P. The Fundamental Plane of Black Hole Accretion and Its Use as a Black Hole-Mass Estimator. *Astrophys. J.* **2019**, *871*, 80.
22. van den Bosch, R.C.E.; Gebhardt, K.; Gültekin, K.; Yıldırım, A.; Walsh, J.L. Hunting for Supermassive Black Holes in Nearby Galaxies With the Hobby-Eberly Telescope. *Astrophys. J. Suppl. Ser.* **2015**, *218*, 10.
23. Makarov, D.; Prugniel, P.; Terekhova, N.; Courtois, H.; Vauglin, I. HyperLEDA. III. The catalogue of extragalactic distances. *Astron. Astrophys.* **2014**, *570*, A13. [CrossRef]
24. Caramete, L.I.; Biermann, P.L. The Mass Function of Nearby Black HOLE Candidates. *Astron. Astrophys.* **2010**, *521*, A55.
25. Mezcua, M.; Hlavacek-Larrondo, J.; Lucey, J.R.; Hogan, M.T.; Edge, A.C.; McNamara, B.R. The Most Massive Black Holes on the Fundamental Plane of Black Hole Accretion. *Mon. Not. R. Astron. Soc. Lett.* **2018**, *474*, 1342–1360.
26. Shaw, M.S.; Romani, R.W.; Cotter, G.; Healey, S.E.; Michelson, P.F.; Readhead, A.C.S.; Richards, J.L.; Max-Moerbeck, W.; King, O.G.; Potter, W.J. Spectroscopy of Broad-line Blazars from 1LAC. *Astrophys. J.* **2012**, *748*, 49.
27. Chen, Y.Y.; Zhang, X.; Zhang, H.J.; Yu, X.L. Core-Dominance Parameter, Black Hole Mass and Jet-Disc Connection for Fermi blazars. *Mon. Not. R. Astron. Soc. Lett.* **2015**, *451*, 4193–4206.
28. Cutri, R.M.; Wright, E.L.; Conrow, T.; Fowler, J.W.; Eisenhardt, P.R.M.; Grillmair, C.; Kirkpatrick, J.D.; Masci, F.; McCallon, H.L.; Wheelock, S.L.; et al. VizieR Online Data Catalog: AllWISE Data Release (Cutri+ 2013). *Vizier Online Data Cat.* **2021**, *II*, 328.
29. Cluver, M.E.; Jarrett, T.H.; Hopkins, A.M.; Driver, S.P.; Liske, J.; Gunawardhana, M.L.P.; Taylor, E.N.; Robotham, A.S.G.; Alpaslan, M.; Baldry, I.; et al. Galaxy and Mass Assembly (GAMA): Mid-infrared Properties and Empirical Relations from WISE. *Astrophys. J.* **2014**, *782*, 90.
30. Huchra, J.P.; Macri, L.M.; Masters, K.L.; Jarrett, T.H.; Berlind, P.; Calkins, M.; Crook, A.C.; Cutri, R.; Erdoğdu, P.; Falco, E.; et al. The 2MASS Redshift Survey—Description and Data Release. *Astrophys. J. Suppl. Ser.* **2012**, *199*, 26.

31. Schutte, Z.; Reines, A.E.; Greene, J.E. The Black Hole-Bulge Mass Relation Including Dwarf Galaxies Hosting Active Galactic Nuclei. *Astrophys. J.* **2019**, *887*, 245.
32. Massaro, E.; Maselli, A.; Leto, C.; Marchegiani, P.; Perri, M.; Giommi, P.; Piranomonte, S. The 5th Edition of the Roma-BZCAT. A Short Presentation. *Astrophys. Space Sci.* **2015**, *357*, 75.
33. Véron-Cetty, M.P.; Véron, P. A catalogue of quasars and active nuclei: 13th edition. *Astron. Astrophys.* **2010**, *518*, A10. [CrossRef]
34. Flesch, E.W. The Half Million Quasars (HMQ) Catalogue. *PASA* **2015**, *32*, e010.
35. Tully, R.B.; Rizzi, L.; Shaya, E.J.; Courtois, H.M.; Makarov, D.I.; Jacobs, B.A. The Extragalactic Distance Database. *Astron. J.* **2009**, *138*, 323–331. [CrossRef]
36. Kim, J.Y.; Krichbaum, T.P.; Broderick, A.E.; Wielgus, M.; Blackburn, L.; Gómez, J.L.; Johnson, M.D.; Bouman, K.L.; Chael, A.; Akiyama, K.; et al. Event Horizon Telescope imaging of the archetypal blazar 3C 279 at an extreme 20 microarcsecond resolution. *Astron. Astrophys.* **2020**, *640*, A69. [CrossRef]
37. Janssen, M.; Falcke, H.; Kadler, M.; Ros, E.; Wielgus, M.; Akiyama, K.; Baloković, M.; Blackburn, L.; Bouman, K.L.; Chael, A.; et al. Event Horizon Telescope Observations of the Jet Launching and Collimation in Centaurus A. *Nat. Astron.* **2021**, *5*, 1017–1028.
38. Issaoun, S.; Wielgus, M.; Jorstad, S.; Krichbaum, T.P.; Blackburn, L.; Janssen, M.; Chan, C.k.; Pesce, D.W.; Gómez, J.L.; Akiyama, K.; et al. Resolving the Inner Parsec of the Blazar J1924-2914 with the Event Horizon Telescope. *Astrophys. J.* **2022**, *934*, 145.
39. Nair, D.G.; Lobanov, A.P.; Krichbaum, T.P.; Ros, E.; Zensus, J.A.; Kovalev, Y.Y.; Lee, S.S.; Mertens, F.; Hagiwara, Y.; Bremer, M.; et al. Global Millimeter VLBI Array Survey of Ultracompact Extragalactic Radio Sources at 86 GHz. *Astron. Astrophys.* **2019**, *622*, A92.
40. Lee, S.S.; Lobanov, A.P.; Krichbaum, T.P.; Witzel, A.; Zensus, A.; Bremer, M.; Greve, A.; Grewing, M. A Global 86 GHz VLBI Survey of Compact Radio Sources. *Astron. J.* **2008**, *136*, 159–180.
41. Cheng, X.P.; An, T.; Frey, S.; Hong, X.Y.; He, X.; Kellermann, K.I.; Lister, M.L.; Lao, B.Q.; Li, X.F.; Mohan, P.; et al. Compact Bright Radio-loud AGNs. III. A Large VLBA Survey at 43 GHz. *Astrophys. J. Suppl. Ser.* **2020**, *247*, 57.
42. Lister, M.L.; Aller, M.F.; Aller, H.D.; Hodge, M.A.; Homan, D.C.; Kovalev, Y.Y.; Pushkarev, A.B.; Savolainen, T. MOJAVE. XV. VLBA 15 GHz Total Intensity and Polarization Maps of 437 Parsec-scale AGN Jets from 1996 to 2017. *Astrophys. J. Suppl. Ser.* **2018**, *234*, 12.
43. Helmboldt, J.F.; Taylor, G.B.; Tremblay, S.; Fassnacht, C.D.; Walker, R.C.; Myers, S.T.; Sjouwerman, L.O.; Pearson, T.J.; Readhead, A.C.S.; Weintraub, L.; et al. The VLBA Imaging and Polarimetry Survey at 5 GHz. *Astrophys. J.* **2007**, *658*, 203–216.
44. Evans, I.N.; Primini, F.A.; Glotfelty, K.J.; Anderson, C.S.; Bonaventura, N.R.; Chen, J.C.; Davis, J.E.; Doe, S.M.; Evans, J.D.; Fabbiano, G.; et al. The Chandra Source Catalog. *Astrophys. J. Suppl. Ser.* **2010**, *189*, 37–82.
45. Lucchini, M.; Ceccobello, C.; Markoff, S.; Kini, Y.; Chhotray, A.; Connors, R.M.T.; Crumley, P.; Falcke, H.; Kantzas, D.; Maitra, D. Bhjet: A public multi-zone, steady state jet plus thermal corona spectral model. *Mon. Not. R. Astron. Soc.* **2022**, *517*, 5853–5881. [CrossRef]
46. Ricarte, A.; Gammie, C.; Narayan, R.; Prather, B.S. Probing Plasma Phys. Spectr. Index Maps Accreting Black Holes Event Horiz. Scales. *arXiv* **2022**, arXiv:202.02408.
47. Porth, O.; Chatterjee, K.; Narayan, R.; Gammie, C.F.; Mizuno, Y.; Anninos, P.; Baker, J.G.; Bugli, M.; Chan, C.k.; Davelaar, J.; et al. The Event Horizon General Relativistic Magnetohydrodynamic Code Comparison Project. *Astrophys. J. Suppl. Ser.* **2019**, *243*, 26.
48. De Rosa, A.; Vignali, C.; Bogdanović, T.; Capelo, P.R.; Charisi, M.; Dotti, M.; Husemann, B.; Lusso, E.; Mayer, L.; Paragi, Z.; et al. The Quest for Dual and Binary Supermassive Black Holes: A Multi-Messenger View. *New Astron. Rev.* **2019**, *86*, 101525.
49. Gitti, M.; Giroletti, M.; Giovannini, G.; Feretti, L.; Liuzzo, E. A Candidate Supermassive Binary Black Hole System in the Brightest Cluster Galaxy of RBS 797. *Astron. Astrophys.* **2013**, *557*, L14.
50. Bansal, K.; Taylor, G.B.; Peck, A.B.; Zavala, R.T.; Romani, R.W. Constraining the Orbit of the Supermassive Black Hole Binary 0402+379. *Astrophys. J.* **2017**, *843*, 14.
51. An, T.; Zhang, Y.; Wang, A.; Shu, X.; Yang, H.; Jiang, N.; Dou, L.; Pan, Z.; Wang, T.; Zheng, Z. VLBI Imaging of the Pre-Coalescence SMBHB Candidate SDSS J143016.05+230344.4. *Astron. Astrophys.* **2022**, *663*, A139.
52. Graham, M.J.; Djorgovski, S.G.; Stern, D.; Drake, A.J.; Mahabal, A.A.; Donalek, C.; Glikman, E.; Larson, S.; Christensen, E. A Systematic Search for Close Supermassive Black Hole Binaries in the Catalina Real-Time Transient Survey. *Mon. Not. R. Astron. Soc. Lett.* **2015**, *453*, 1562–1576.
53. Ren, H.X.; Cerruti, M.; Sahakyan, N. Quasi-Periodic Oscillations in the γ-ray Light Curves of Bright Active Galactic Nuclei. *arXiv* **2022**, arXiv:2204.13051.
54. Severgnini, P.; Braito, V.; Cicone, C.; Saracco, P.; Vignali, C.; Serafinelli, R.; Della Ceca, R.; Dotti, M.; Cusano, F.; Paris, D.; et al. A possible sub-kiloparsec dual AGN buried behind the galaxy curtain. *Astron. Astrophys.* **2021**, *646*, A153.
55. Terwel, J.H.; Jonker, P.G. Discovery of a Quasar with Double-Peaked Broad Balmer Emission lines. *Mon. Not. R. Astron. Soc. Lett.* **2022**, *512*, L80–L84.
56. Saripalli, L.; Roberts, D.H. What Are "X-shaped" Radio Sources Telling Us? II. Properties of a Sample of 87. *Astrophys. J.* **2018**, *852*, 48. [CrossRef]

57. Mingarelli, C.M.F.; Lazio, T.J.W.; Sesana, A.; Greene, J.E.; Ellis, J.A.; Ma, C.P.; Croft, S.; Burke-Spolaor, S.; Taylor, S.R. The Local Nanohertz Gravitational-Wave Landscape from Supermassive Black Hole Binaries. *Nat. Astron.* **2017**, *1*, 886–892.
58. Bower, G.C.; Dexter, J.; Markoff, S.; Gurwell, M.A.; Rao, R.; McHardy, I. A Black Hole Mass-Variability Timescale Correlation at Submillimeter Wavelengths. *Astrophys. J. Lett.* **2015**, *811*, L6.